문서번호 APCC-출장-16-0995(2016-09-21)

| 결재 | 선임연구원 | 팀장 | 팀장 | 부서장 |
|---|---|---|---|---|
| | 09/20<br>Vladimir Kryjov | 09/21<br>이우섭 | 대결 09/21<br>김선태 | 대결 09/21<br>김형진 |
| 협조 | | | | |
| | | | | |

# TRAVEL REPORT FORM
# 출장보고서

## I. Reporter 보고자

| Department<br>소속 | Position<br>직위(직급) | Name<br>성명 | Travel Date<br>날짜 | Note<br>비고 |
|---|---|---|---|---|
| Climate Prediction Team | Research Fellow | Vladimir Kryjov | 2016/9/11~9/17 | |

## II. Major Activities 주요업무 수행내용

1. Main Contents and Activities 주요내용 및 활동

- Oral presentation "Synoptic Aspects of Predictability of the Wintertime Arctic Oscillation"
- Poster presentation "Skill of Real-Time APCC's Seasonal Muloti-Model Ensemble Predictions during the Period 2008 – 2014".

2. Relevance to APEC Climate Center's Activities 결론 및 소감

Both presentations are directly related to APCC's activity

## III. References 참고사항

(with attachment of any information or report in case of attendance of conferences, workshops and meetings) 학술대회, 워크숍, 회의 등 참석 시 관련 정보 및 문서 첨부

1. Presented and Collected Materials 주요 수집자료

2. Suggestions and Remarks 건의사항

# Synoptic Aspects of Predictability of the Wintertime Arctic Oscillation

Vladimir Kryjov, Young-Mi Min

APEC Climate Center
Busan, Republic of Korea

# Introduction

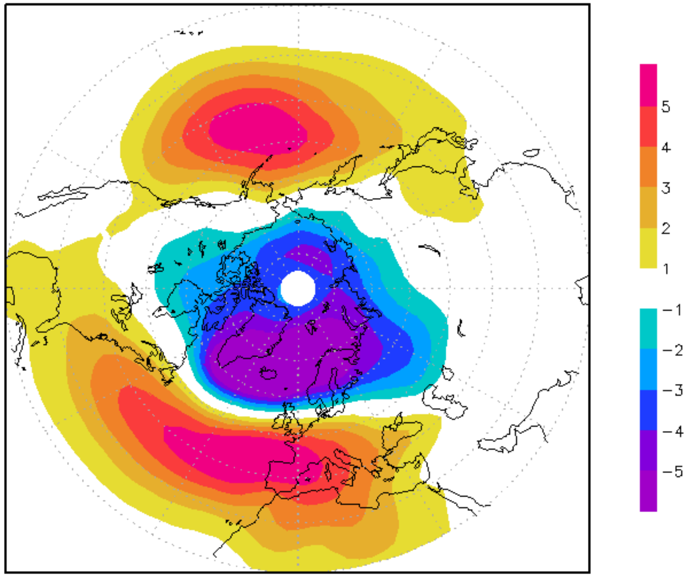


EOF1 (19%) of the mean monthly Z1000 anomalies (1979–2000).

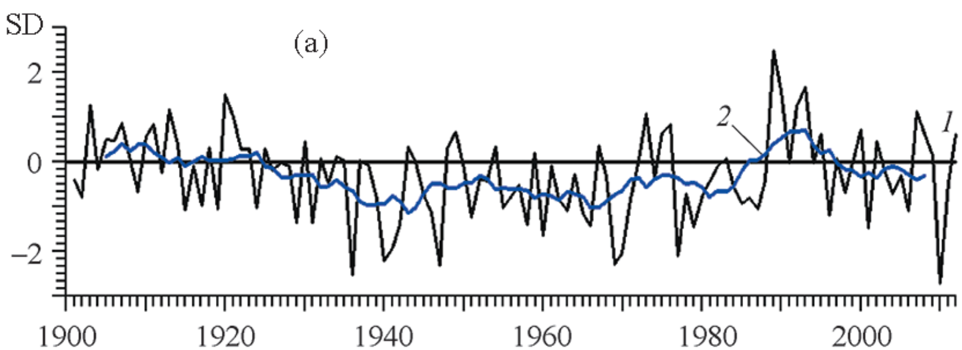


Time series of the normalized wintertime (December–March) AO index (*1*), and its 9-year running mean (*2*)

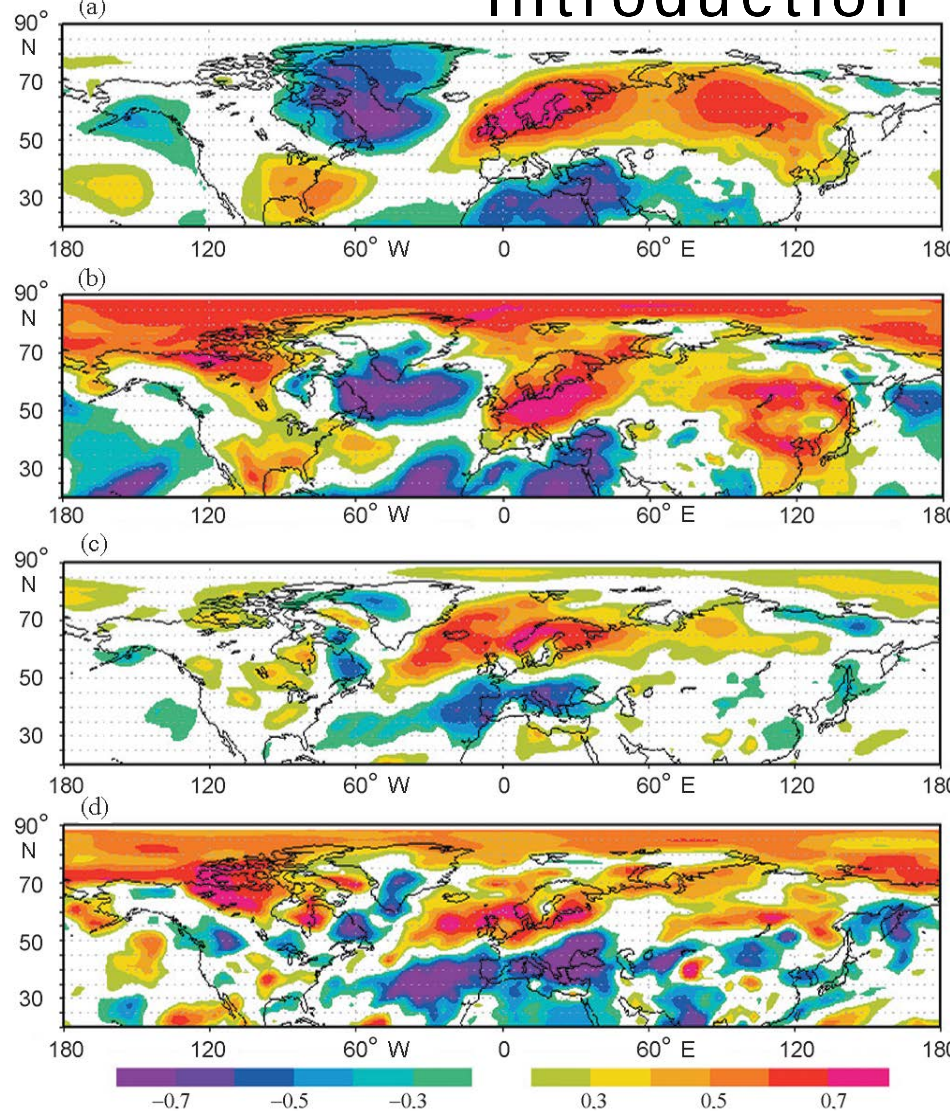


Correlations between the high frequency (a, c) and low frequency (b, d) components of the mean wintertime (December–March) values of (a, b) air temperature, (c, d) total precipitation, and the AO index (1905–2008).

# Current level of predictability of the wintertime AOI
## (operational seasonal climate prediction models, one month lead)

•**Most common:** correlation < **0.2** on 20 - 30-year series.

•**Highest:**

-GloSea5 (14-year series): correlation **0.63**
(Scaife et al., 2014, MacLachlan et al., 2014).

- PNU (30-year series): correlation **0.60**
(Ahn and Kim, 2013; Sun and Ahn, 2014).

- CMCC (30-year series): correlation **0.55**
(Athanasiadis et al.,2014; Materia, 2016 (talk at APCC)).

**That is, seasonal predictions of the most successful state-of-the-art models explain up to 30-40% of the variance of the wintertime AOI.**

## Mechanism of the lag AO response to autumn influence beyond empirical studies

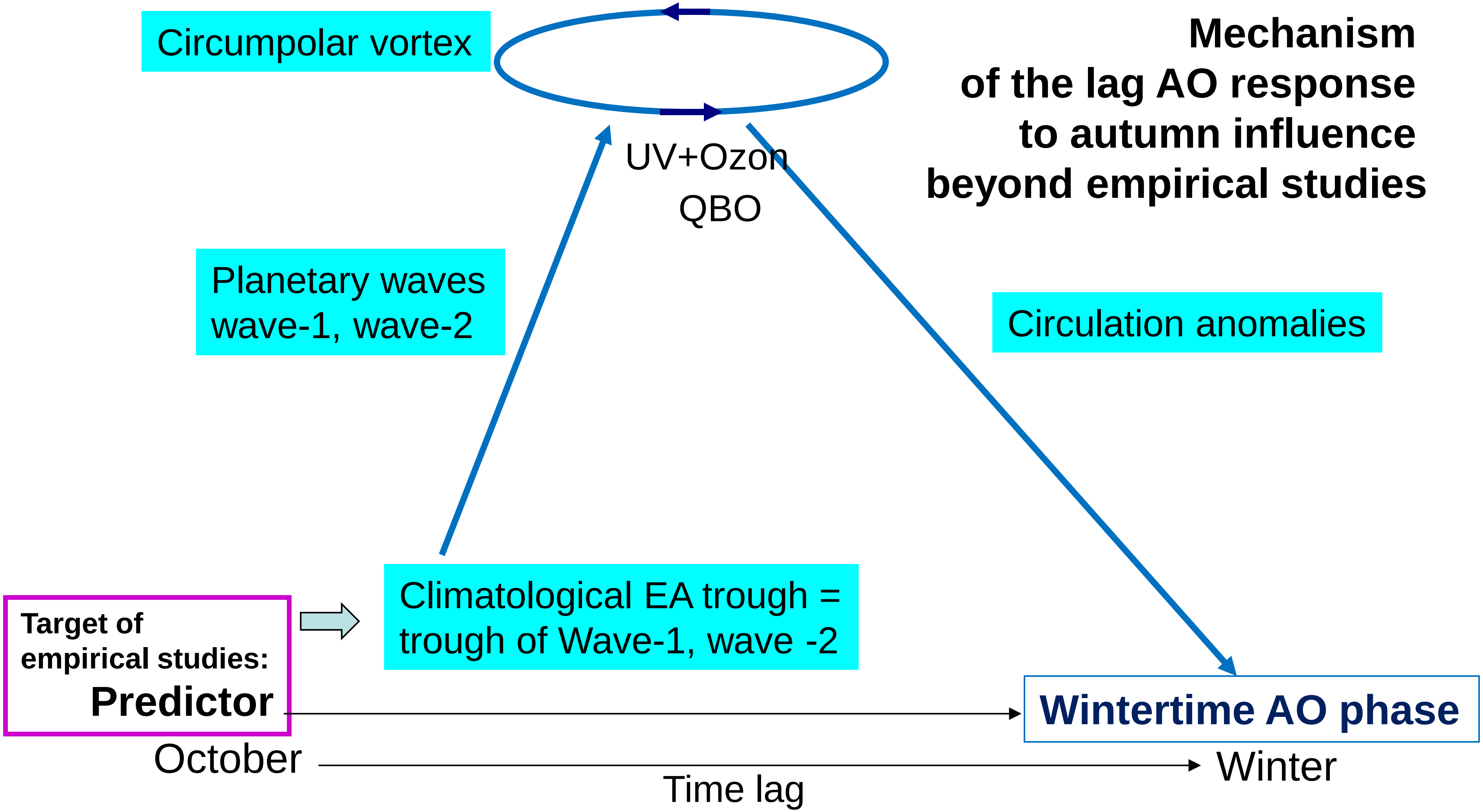


**Mechanism description:**
Theoretical: Charney and Drazin, 1961; Haynes et al., 1991; and others
Modelling: Shindel et al., 2001; Fletcher and Kushner, 2011, and others
Empirical: Baldwin and Dunkerton, 1999; Limpasuvan et al., 2005; Cohen et al., 2010, and others

## Mechanism of the lag AO response to autumn influence

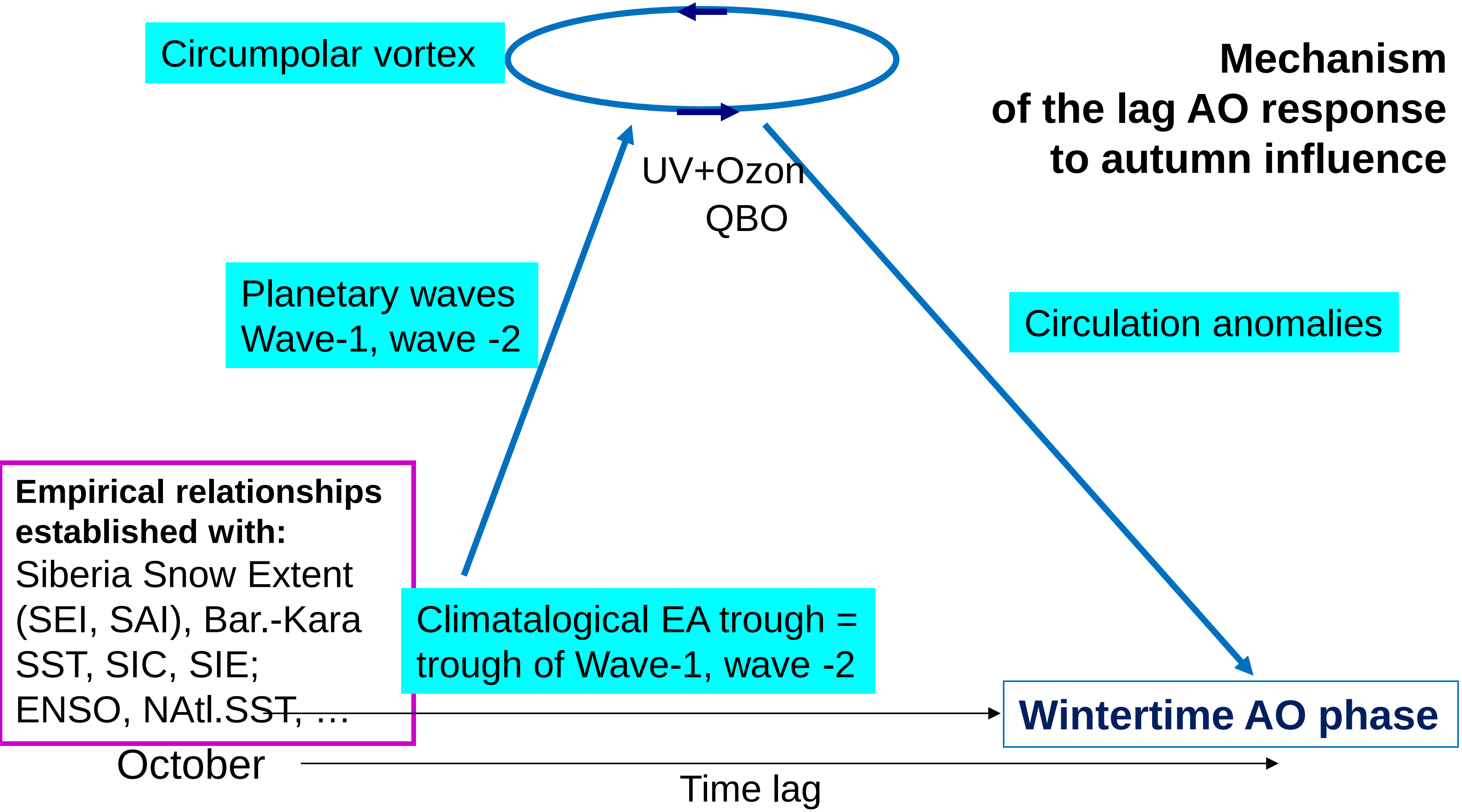


**Empirical relationships:**
Cohen et al., 2007; Cohen and Jones, 2011; Garfinkel et al., 2010; Deser et al. 2010; Liu et al. 2012; Folland et al., 2012; Scaife et al., 2014, Hall et al., 2015; Kryjov, 2015; and others

October **TCI** (Z700 anomaly over the Taymyr Peninsula) yields a correlation of **0.58** with the DJF AO index on **dependent** 55-year series (Kryjov, 2015)

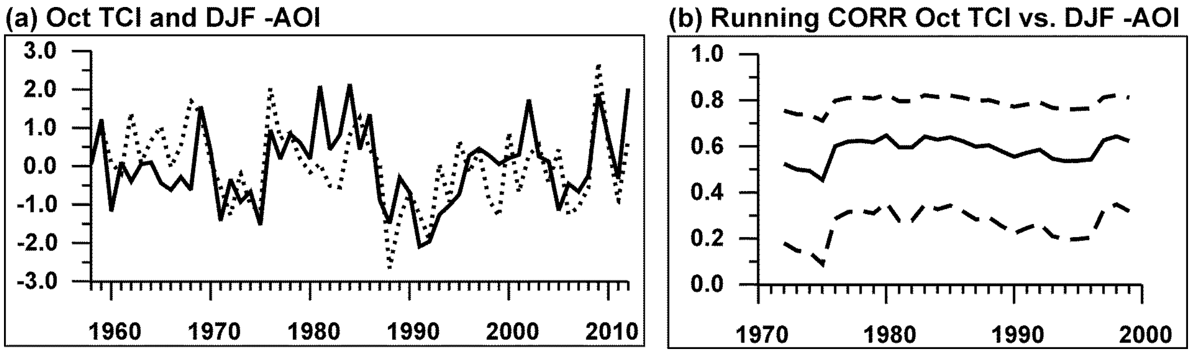


(a) Time series of October TCI (solid line) and inverted DJF AOI (dots), with both series normalized with respect to a 1958 - 2012 base period. R=0.58
(b) Running correlations calculated over 27 yr. windows (plotted in central year of 27 yr. periods) between October TCI and inverted DJF AOI (solid) and their 95% confidence intervals (dashed)

**In the next study** (Kryjov & Min, 2016) **this relationship is tested in a prediction mode on (quasi-)independent data and yeilds quite optimistic results.**

**This presentation shows results from these studies focusing on the synoptic processes underlying predictability of the wintertime AO.**

# Data and Method of Prediction

# Data

Reanalysis I: SLP, ZXXXs,

Reanalysis II: T2m

20CR: Precipitation, Snow cover

HISST: SST, SIC

55 winters: 1958/59 – 2012/13

# Time structure of the performed experiment

## Simulation of real-time forecast procedures

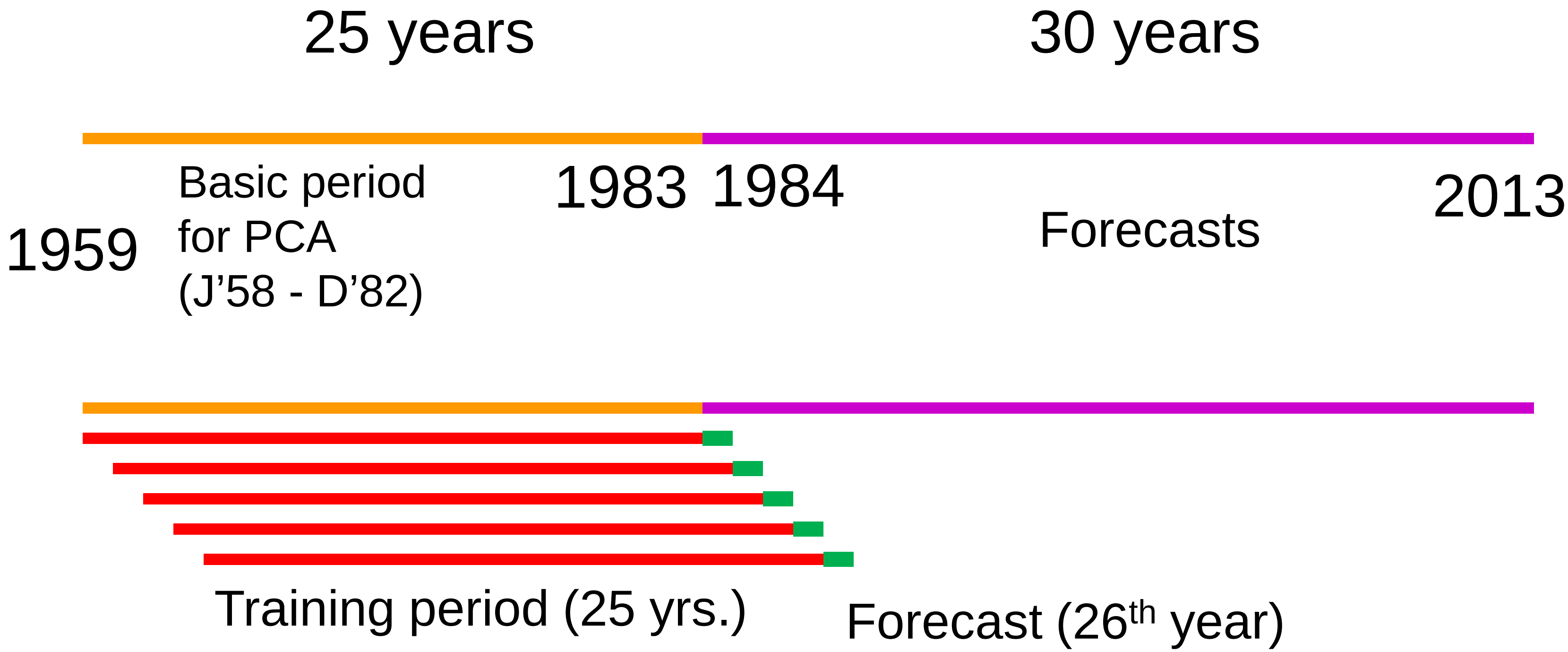


Total: 30 forecasts with a 1 year increment

Year as of January (e.g., the 1959 mark corresponds to D'58 – F'59)

# Method of each year forecast

1. Oct. Z500 N of 20N 25 yrs. × 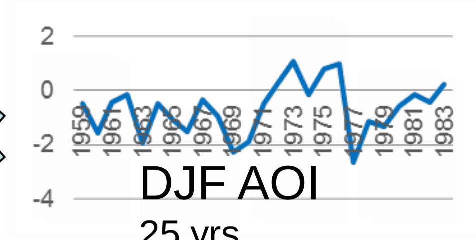

DJF AOI 25 yrs. → Corr. Map N of 20N

2. Oct. Z500 25 yrs. × Corr. map → 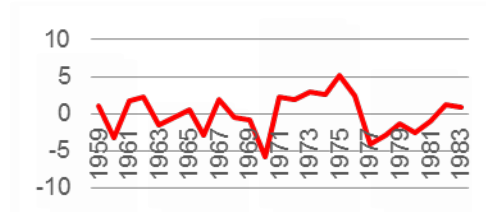

Predictor 25 yrs.

**No restrictions on corr. value**

3. 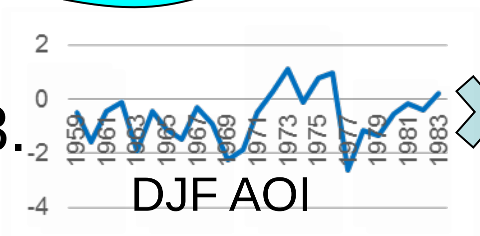

DJF AOI × 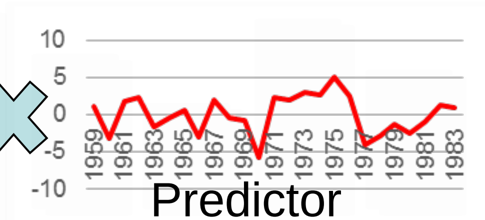

Predictor → DJF_AOI = a + b * Predictor

4. Oct. Z500 $26^{th}$ yr. × Corr. map → Predictor(yr.=26)

5. **Forecast: DJF_AOI(yr.=26) = a + b * Predictor(yr.=26)**

# Prediction resulta

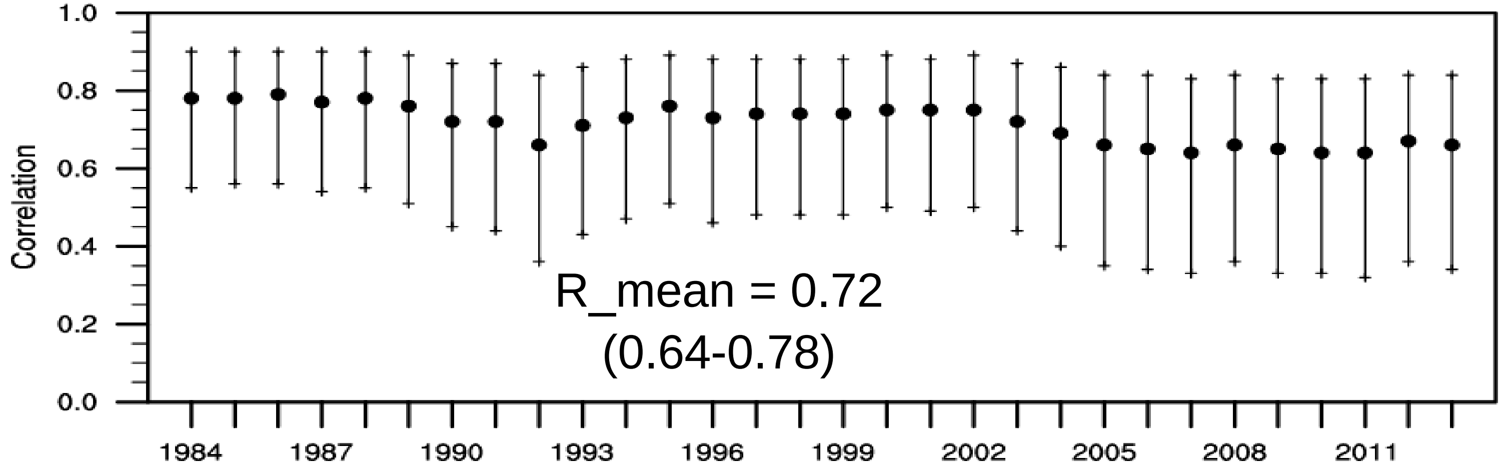


**Predictors:** Correlations between the constructed predictors and the wintertime AOI for the sliding 25-year training periods plotted at the forecast years

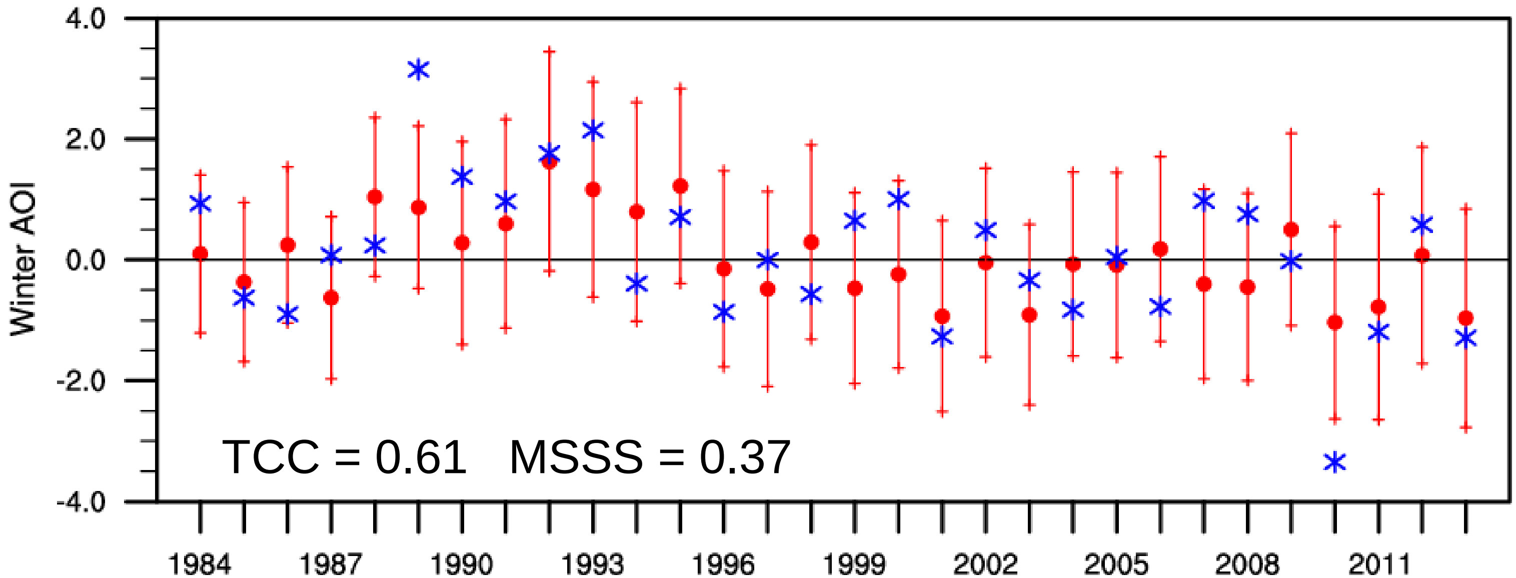


**Result: DJF AOI: Observations (blue), Forecasts (red)**

(Kryjov & Min, 2016)

What is beyond?

# Summary of the correlation maps

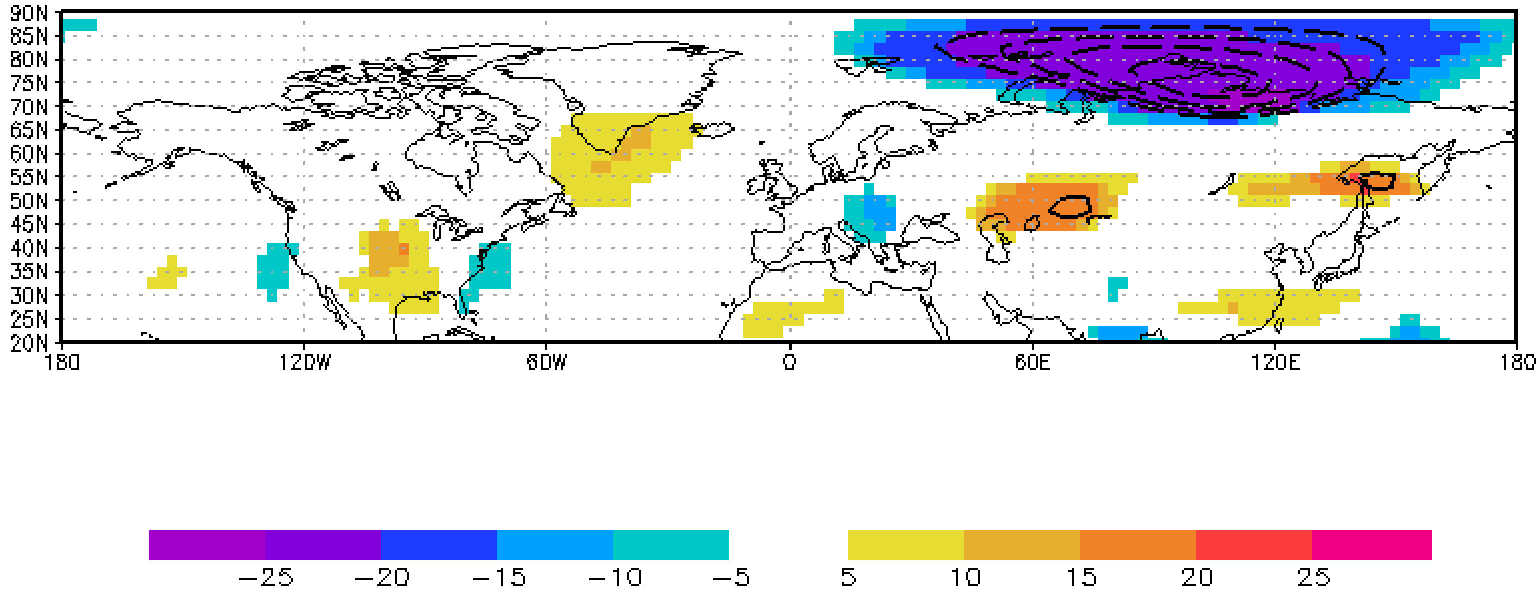


**Shading:** The number of forecasts (out of 30) with absolute value of correlation coefficients between the DJF AO and gridpoint series of Z500 during the training period being above 0.4. The sign corresponds to the sign of 30-yr average correlation.

**Contours:** mean correlation coefficients between the DJF AO and constructed predictors (correlations underlying regression). Values between -0.3 and +0.3 are omitted.

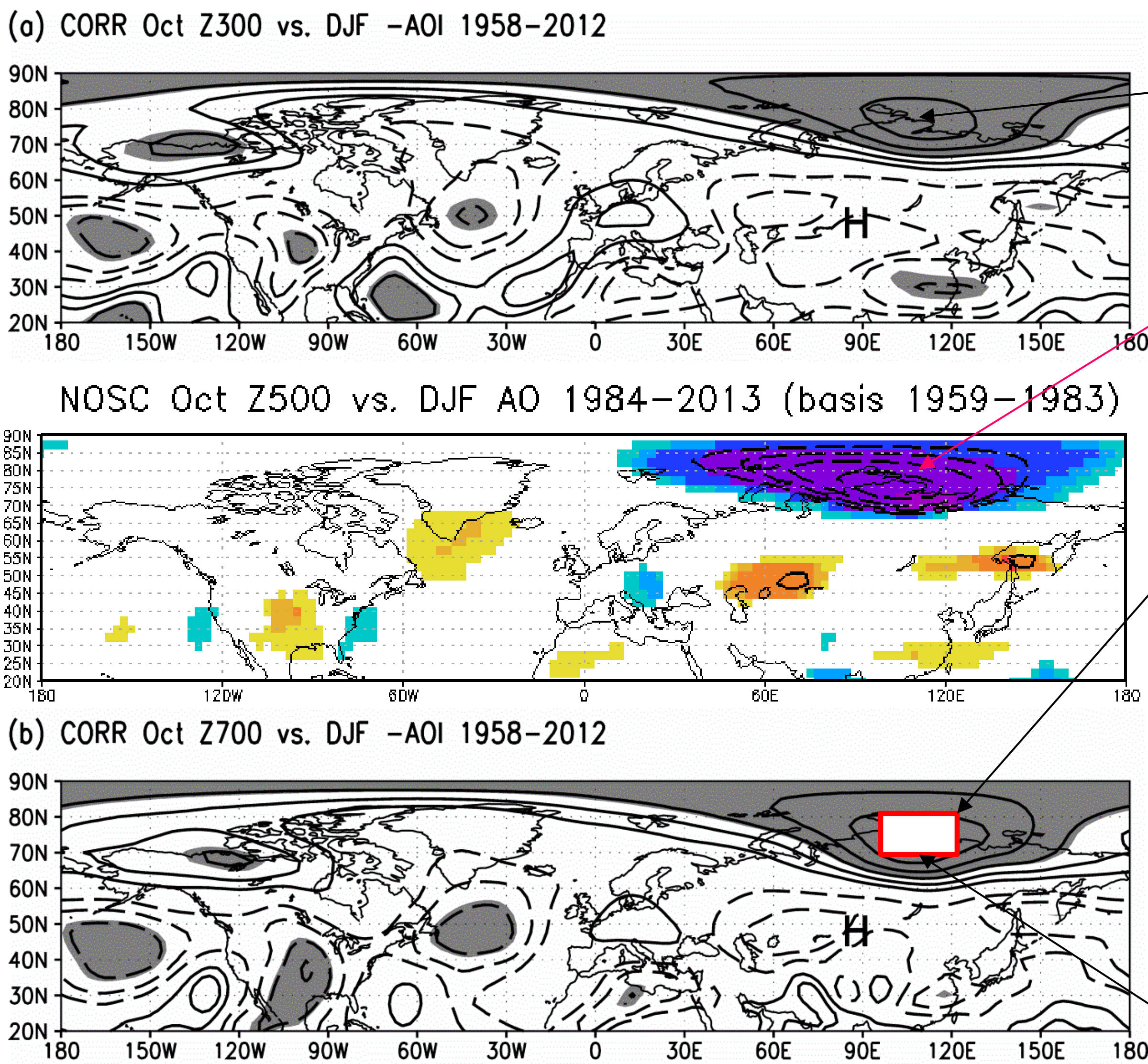


TCA

Correlations between
October Z300 (a),
Z700 (b),
SLP (c)
and the inverted DJF AOI
for 1958 - 2012.

Contour interval is 0.1, negative values are dashed, the 0 value is omitted. The area where the correlations are significant at the 5% level in a two-tailed test is shaded

Definition of TCI
(80-70N, 100-120E)

B&W figures from Kryjov (2015)

# Illustration corresponds to Oct TCA+ and DJF AO-

**Positive tropospheric temperature anomaly**

**Climatological East Asia Trough (wave-1 & wave-2)**

**Negative tropospheric temperature anomaly**

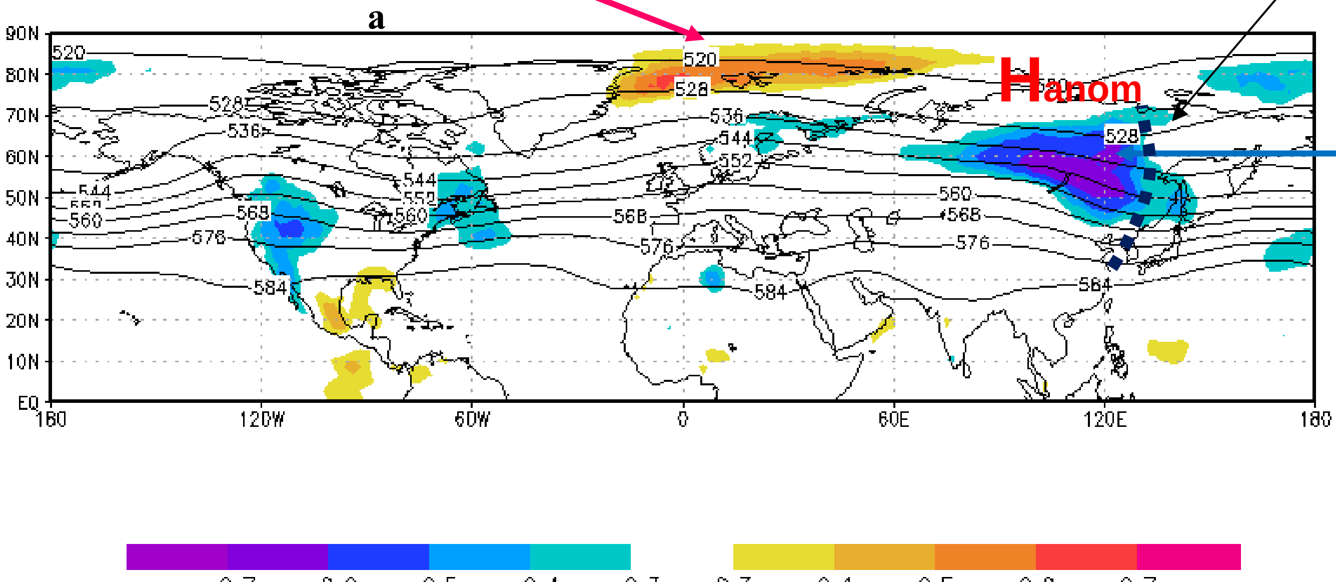


**Correlations between October T2m and TCI. (1979-2010). Contours – Z500 climatology.**

# Illustration corresponds to Oct TCA+ and DJF AO-

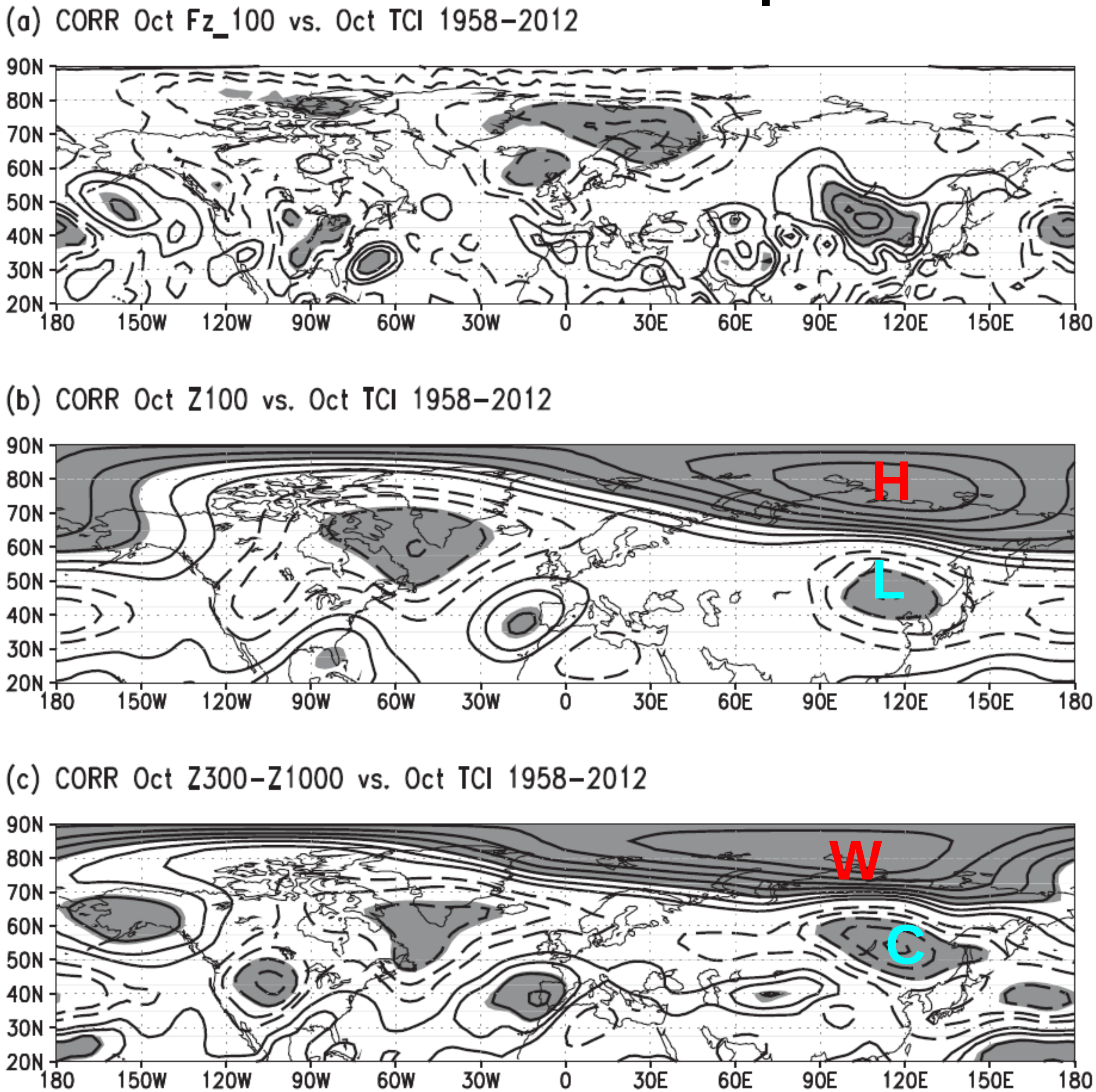


Correlations between the October upward 100-hPa EP flux (a), Z100 (b), 300-1000-hPa layer thickness (c) and the October TCI for 1958 - 2012.

Contour interval is 0.1, negative values are dashed, the 0 value is omitted.

The area where the correlations are significant at the 5% level in a two-tailed test is shaded

B&W figures from Kryjov (2015)

# Associated Synoptic Processes and Other Possible Predictors

**Composites of October SLP** (mb)
for winters of the DJF AOI above the upper quintile, below the lower quintile and their difference.

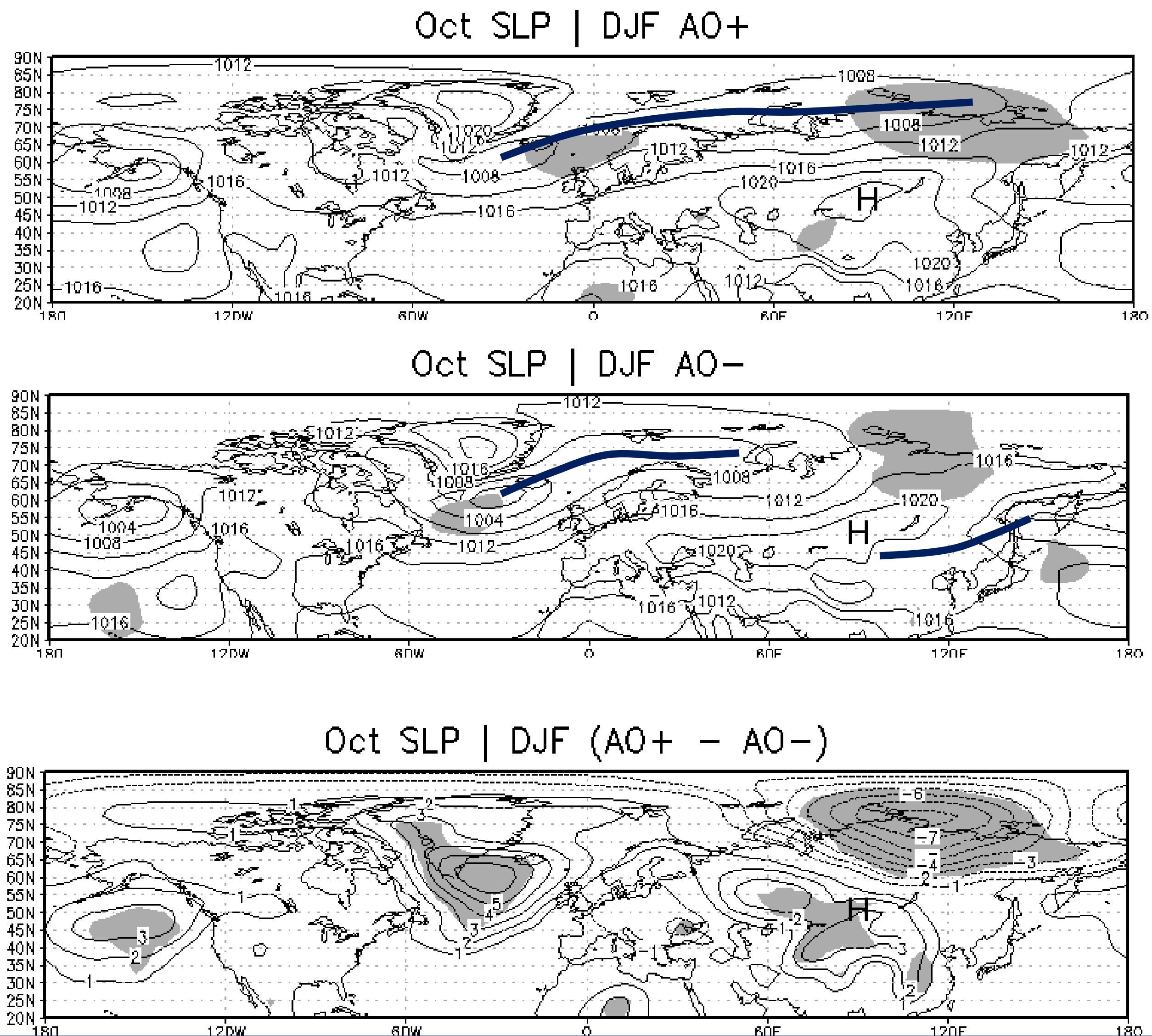


The area where the SLP anomalies and the differences are significant at the 2.5% level in a one-tailed test is shaded.

The letter “H” denotes the October climatological centre of the Siberian High.

Blue bold lines show the axes of the troughs

# **Composites of October Z500** (m)

for winters of the DJF AOI above the upper quintile, below the lower quintile and their difference.

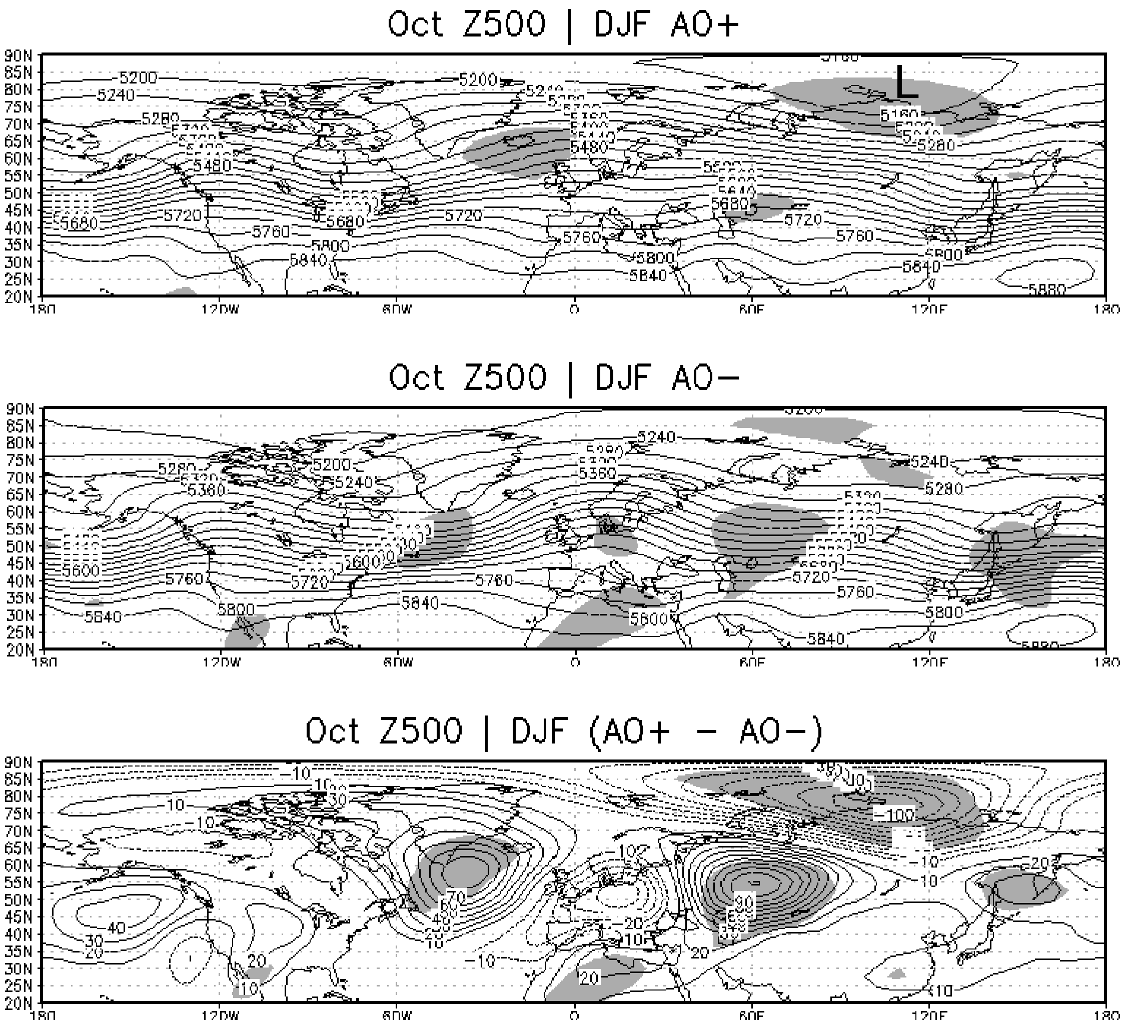


The area where the Z500 anomalies and the differences are significant at the 2.5% level in a one-tailed test is shaded.

The letter “H” denotes the October climatological centre of the Siberian High.

Blue bold lines show the axes of the troughs

# **Composites of October U300** (m/s)

for winters of the DJF AOI above the upper quintile, below the lower quintile and their difference.

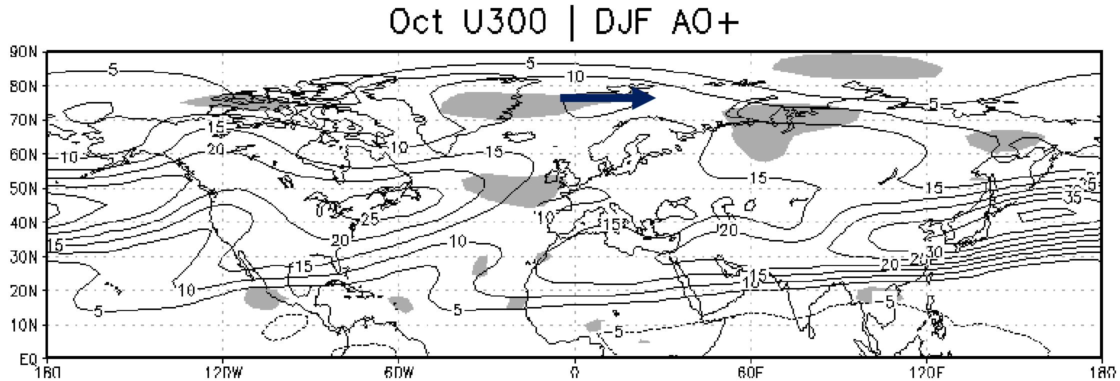


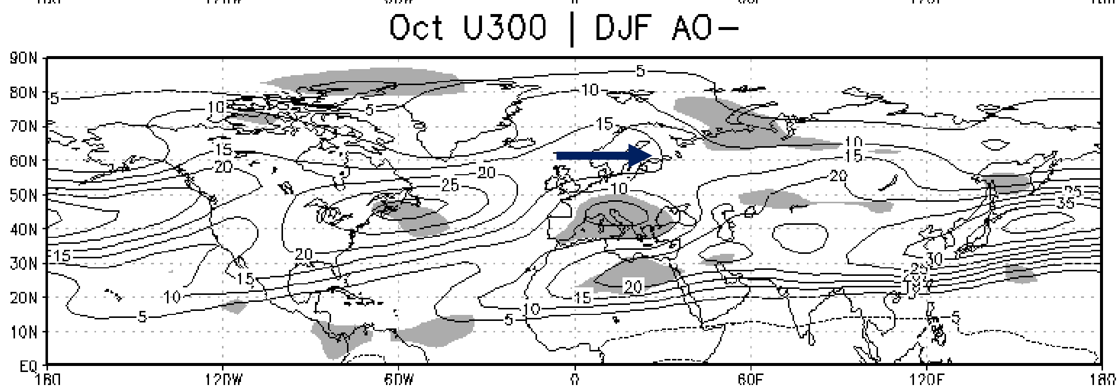


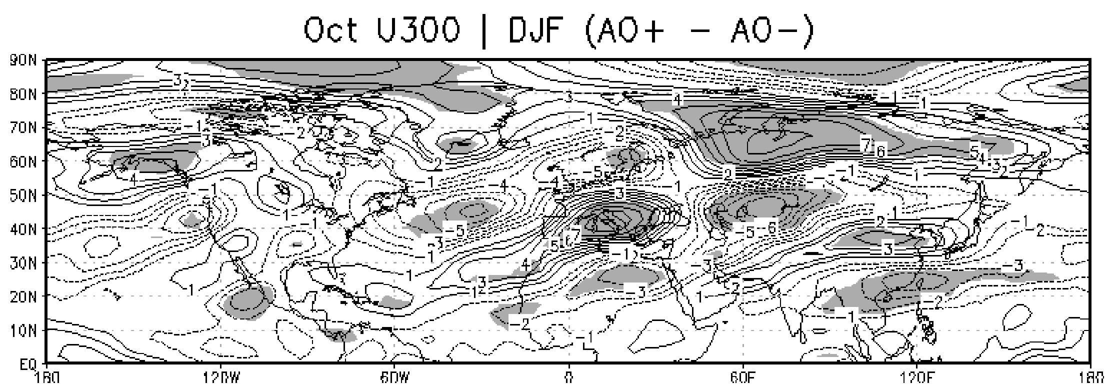

Z500 vs. variable predictors **R_mean**

Regr. **R_mean / TCC**

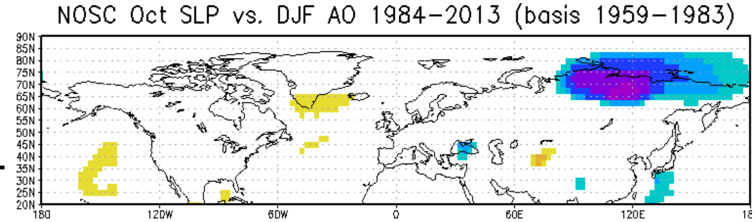


**0.91** **0.63 / 0.40**

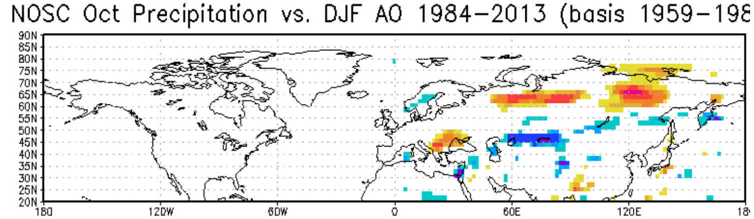


**0.83** **0.91 / 0.26**

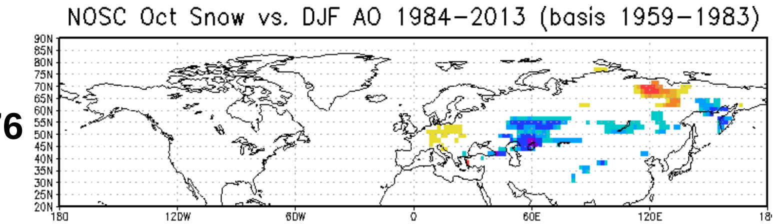


**0.76** **0.79 / 0.40**

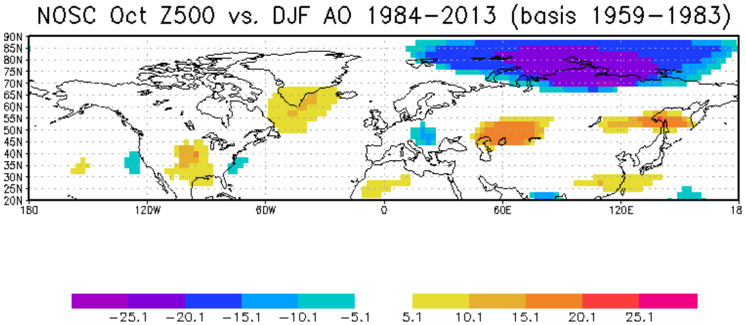


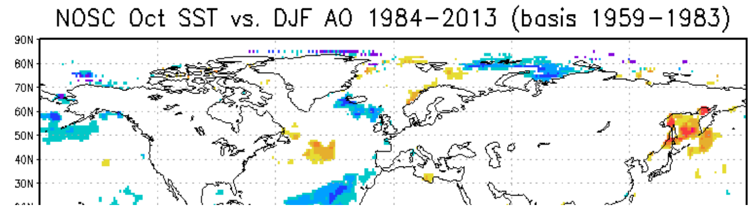


**0.56** **0.71 / 0.31**

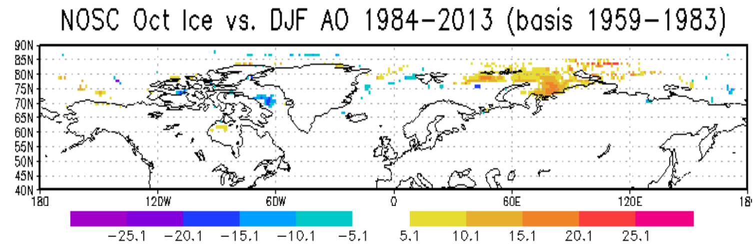


**0.41** **0.79 / 0.32**

The number of years (out of 30) with correlations underlying regression |R|>0.4

Original correlation maps (30 maps) estimated 30 times based on sliding 25-year training periods

# Conclusions

October Z500 successful predictor patterns tend to resemble a pattern of the Taymyr Circulation Anomaly.

A mechanism linking the DJF AO phase with October circulation is anomalous October heat advection of different signs to the Arctic and to the East Asia.

October synoptic processes preceding the DJF positive AO phase are the northward shift of the PJS, enhancement of Z500 steering flow over the northernmost Eurasia, propagation of Atlantic cyclones up to Taymyr Peninsula and the Laptev sea. Vice versa for DJF negative AO phase.

Assessments based on the series of 30 independent predictions of the wintertime AO reveal correlation between the predicted and observed DJF AOI exceeding 0.6 and MSSS exceeding 0.35.

The carried out analysis yields that seasonal prediction may be based on a certain succession of rapidly varying atmospheric processes starting from certain initial conditions, not only on the slowly varying boundary conditions.

Thank you

PCC of the APCC single-model (symbols) and SCM MME predictions (red solid line) for temperature over (a) globe, (b) northern extratropics, (c) tropics, and (d) southern extratropics for the period JFM 2008 ~ DJF 2014/15. Dashed lines indicate the average of all single-model's PCCs. The values in the brackets are the PCC values of the SCM predictions averaged over the whole period for each region.

# Skill of Real-Time APCC's Seasonal Multi-Model Ensemble Predictions during the period 2008-2015


**Young-Mi Min[1], Vladimir N. Kryjov[1]**

[1] APEC Climate Center, Busan, Repub. of Korea (E-mail: ymmin@apcc21.org)


## 1. Introduction

❖ **The Asia-Pacific Economic Cooperation Climate Center (APCC)** has been issuing real-time global forecasts of temperature and precipitation since November 2007. Nowadays, 16 state-of-the-art models from the leading climate centers and research institutes from 10 countries are involved in the APCC operational MME prediction (Min et al. 2014).

❖ The purpose of this study is **to assess an overall performance of the current APCC operational prediction system based on its real-time seasonal forecasts for the period 2008-2015.** It is very important from an operational perspective to assess ability of the APCC MME prediction system on the data from the period not overlapping with the period of hindcasts.

## 2. Data

❖ **Period**: 23-year retrospective (1981-2003) and 8-year real-time (2008-2015) forecasts
❖ **Target**: monthly 3-month mean (seasonal) mean temperature and precipitation
❖ **Observation** for verification: CAMS-OPI for precipitation, NCEP/NCAR Reanalysis II for temperature

| Model | Organization/Country | Resolution | Ens Size (H/F) | Reference |
|---|---|---|---|---|
| CCSM3 | APCC/Korea | T85L26 | 10/10 | Jeong et al. (2008) |
| BCC | BCC/China | T42L18 | 8/8 | Ding et al. (2000) |
| CMCC | CMCC/Italy | T63L19 | 9/9 | Alesandri et al. (2010) |
| COLA | COLA/USA | 1.875x1.865deg L18 | 10/10 | Collins et al. (2006) |
| CWB | CWB/Chinese Taipei | T42L18 | 10/10 | Liou et al. (1997) |
| GloSea5 | KMA⁷/Korea | 0.83x0.56deg L85 | 12/42 | Kang et al. (2011) |
| HMC | HMC/Russia | 1.125x1.406deg L28 | 10/10 | Trosnikov et al. (2005) |
| IRI | IRI/USA | T42L19 | 24/24 | Barnston et al. (2003) |
| JMA | JMA/Japan | T95L40 | 5/51 | Takaya et al. (2010) |
| MGO | MGO/Russia | T42L14 | 6/10 | Shneerov et al. (2002) |
| CANCM3 | MSC/Canada | T63L31 | 10/10 | Scinocca et al. (2008) |
| CANCM4 | MSC/Canada | T63L31 | 10/10 | Merryfield et al. (2013) |
| GMAO | NASA/USA | 288x181grid L72 | 11/11 | Molod et al. (2012) |
| CFSv2 | NCEP/USA | T62L64 | 20/20 | Saha et al. (2014) |
| PNU | PNU/Korea | T42L18 | 10/10 | Ahn and Kim (2013) |
| POAMA | BOM/Australia | T47L17 | 33/33 | Lim et al. (2012) |
| GloSea5 | UKMO/UK | 1.875x1.25deg L85 | 12/42 | MacLachlan et al.(2015) |

## 3. Performance of Deterministic Forecast

➢ **This deterministic forecast is a simple composite of ensemble means (SCM) of participating models.**

❍ **General Performance**

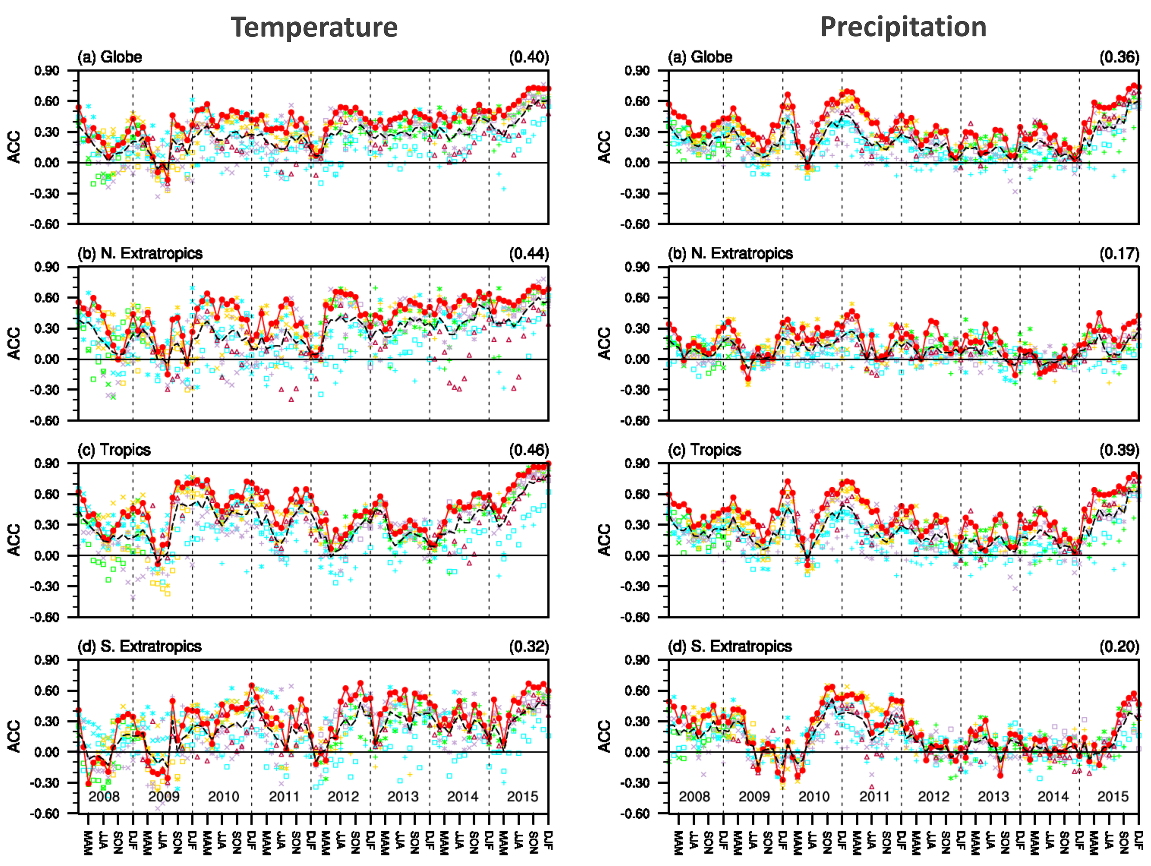


**Fig. 1** PCC of the APCC single-model (symbols) and SCM MME predictions (red solid line) for temperature and precipitation over (a) globe, (b) northern extratropics, (c) tropics, and (d) southern extratropics for the period JFM 2008 – DJF 2015/16. Dashed lines indicate the average of all single-model's PCCs. The values in the brackets are the PCC values of the SCM predictions averaged over the whole period for each region.

❍ **Spatial Distribution**

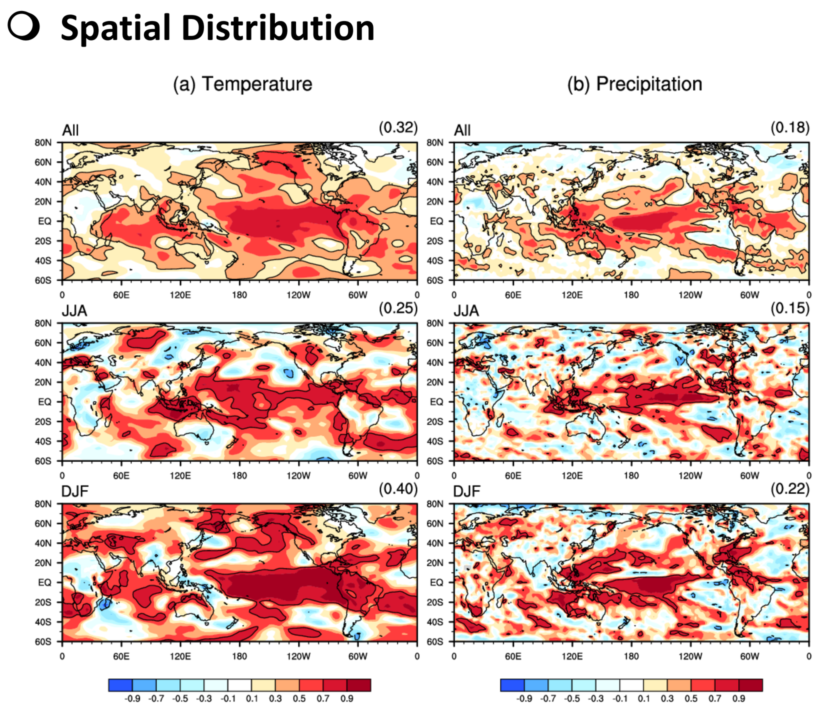


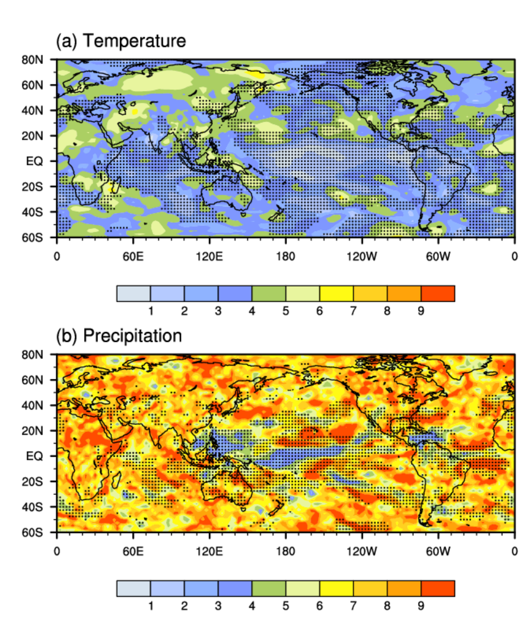


**Fig. 2** Spatial distribution of TCC for the SCM predictions of (a) temperature and (b) precipitation for 96 forecasts, for eight JJA and DJF forecasts for the period 2008-15. The area-averaged scores over the globe are displayed in the brackets. The contour lines enclose the areas where the TCC is statistically significant at the 5% level using the two-tailed Student's t-test.

**Fig. 3** The difference between the highest and lowest of 12 TCCs, characterizing the skill of seasonal forecasts of (a) temperature and (b) precipitation over the period 2008-15. Dots indicate that the temporal correlation for all seasons during the period is statistically significant at the 5% level using the two-tailed Student t-test.

## 4. Performance of Probabilistic Forecast

➢ The **probabilistic multi-model ensemble** (**PMME**) forecast, presented in the form of tercile-based categorical probabilities, is estimated as a weighted combination of individual model probabilistic forecasts, computed with the use of Gaussian approximation of probability distribution of ensemble members, with model weights being inversely proportional to the random errors in the forecast probability (Min et al. 2009).

❍ **Temporal Variation of forecast skill**

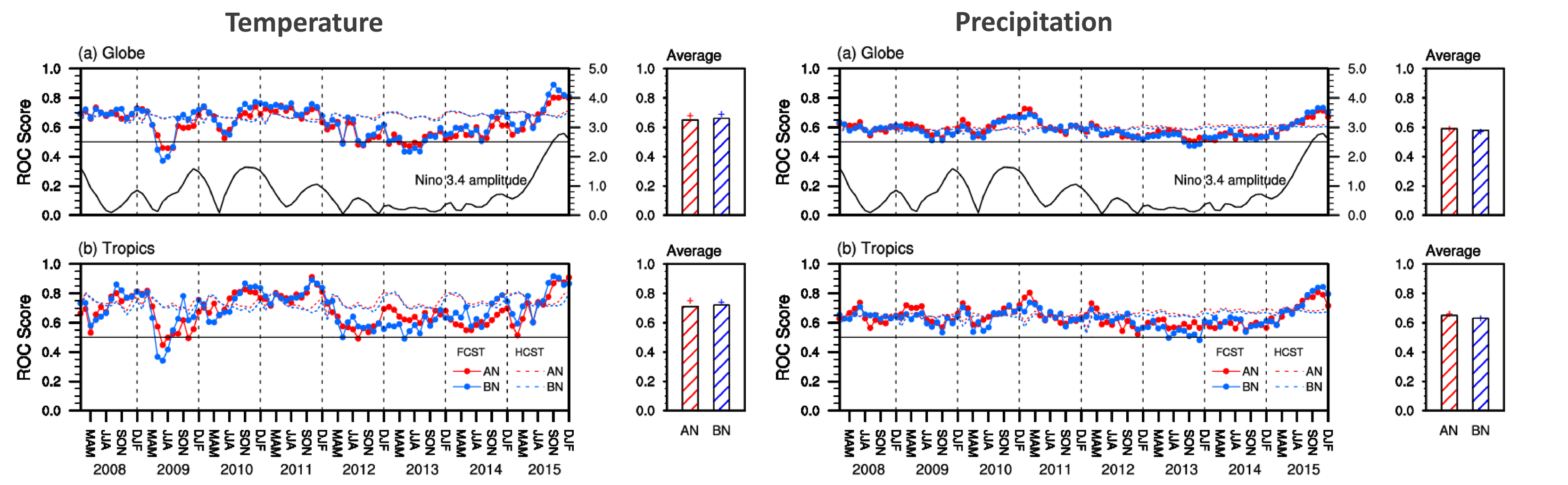


**Fig. 4** Time series of ROC score aggregated over the (a) globe and (b) tropics for PMME prediction for temperature and precipitation (AN; above-normal, BN; below-normal) for the period 2008JFM to 2015/16DJF (FCST). The black line indicates the amplitude (absolute value) of Nino 3.4 index. The 21-year hindcast skill for each category is displayed with a dashed line for comparison (HCST). The averaged scores over the region for the whole series of FCST (bar) and HCST (plus) are also shown.

❍ **Aggregated forecast skill**

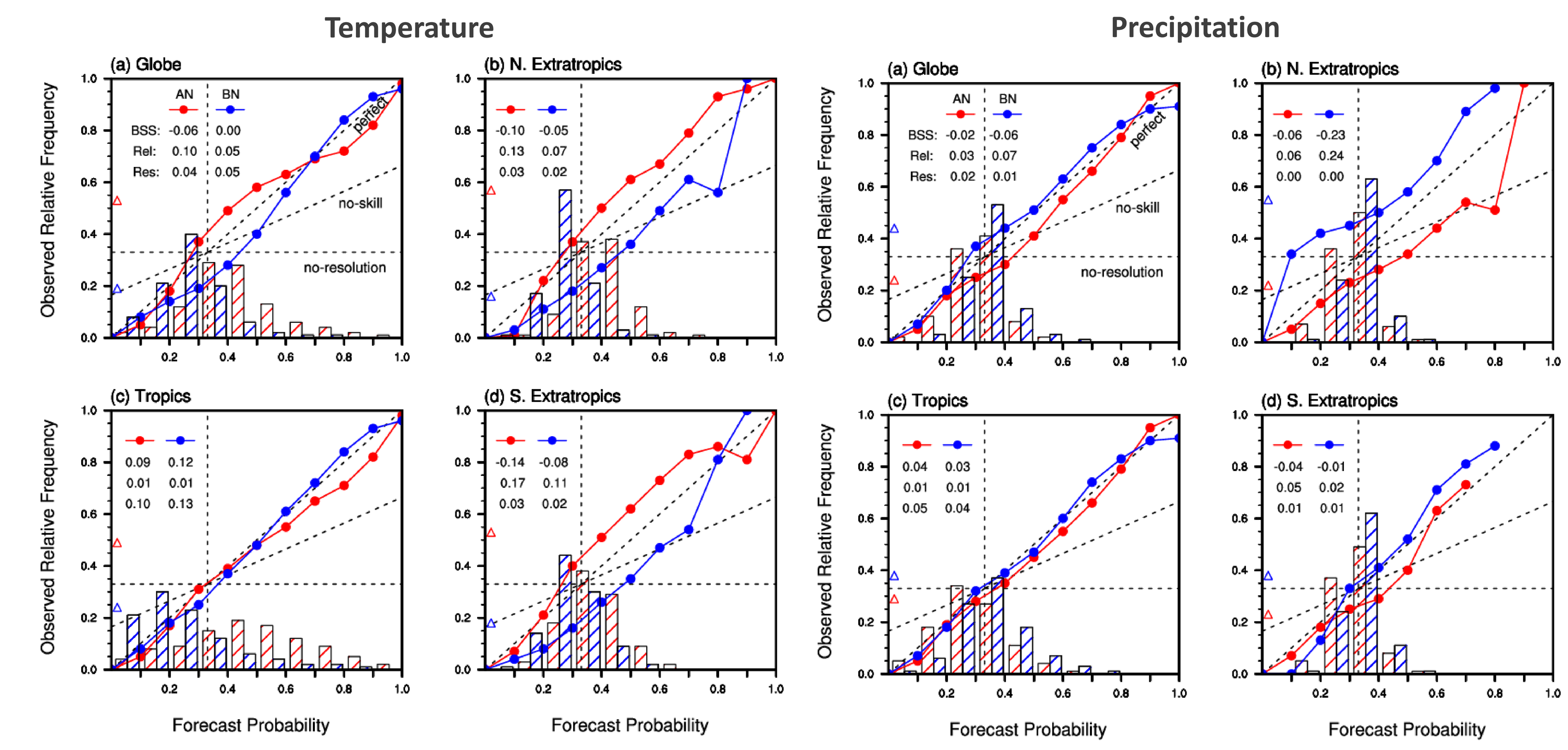


**Fig. 5** Reliability diagrams for the temperature and precipitation forecasts over (a) globe, (b) northern extratropics, (c) tropics, and (d) southern extratropics. Triangle on the vertical axes in red (blue) color indicates the average observed relative frequency of AN (BN) outcome. Also shown is the Brier Skill Score (BSS), including its decomposition in reliability (Brel) and resolution terms (Bres).

## 5. Summary

❖ This study shows performance of the deterministic and probabilistic APCC operational real-time forecasts issued for the period 2008-2015.

❖ **The APCC MME real-time deterministic forecasts during the 8-year period show a reasonably good level of skill**, with the global average TCC being 0.40 for temperature and 0.36 for precipitation (Fig. 1). A skill of the APCC forecasts strongly depends on seasons and regions. It is higher for the tropics and boreal winter than for the extratropics and boreal summer due to direct effects and remote teleconnections from boundary forcings (Fig. 2). The skill improvement by the MME technics is higher for precipitation than for temperature, which could be explained by the higher independence of the individual model errors in precipitation forecasts . The region of the highest improvement by the MME technics is the northern extratropics, as shown by the relative skill improvement (Fig. 3).

❖ During the period 2008-15, the APCC operational PMME prediction system performs properly with the ROC score much higher than 0.5 for all categories, variables, and regions (Fig. 4). However, **the probabilistic temperature forecasts for the 8-year period show the distinct cold bias**, which is evident for all regions (Fig. 5). The deficiency of these forecasts is likely related to the fact that the years considered were substantially warmer than the climatology from 1983-03 base period. This warm condition is clearly manifested in the northern and southern extratropics and is a major feature of the global climate for this period, but it has evidently not anticipated by the APCC multi-model forecasts. **Similar wet bias is also seen for precipitation, particularly for the northern and southern extratropics.** During the period 2008-15, we experienced the drier conditions than during the reference period (1983-2003), but it was not foreseen in the APCC probabilistic multi-model forecasts.

❖ **The level of prediction skill for global and tropical temperature during the 8-year period is slightly less than the average of 21-year hindcast skill whereas precipitation forecast skill is comparable to the hindcast skill** (Fig. 4). Relatively lower skills for both variables tend to occur during most of 2012-14 on the background of the El-Nino-La-Nina transitions or the ENSO-neutral. The highest skill during the whole 8-year period occurs in 2015/16 boreal winter, a peak of the very strong El Nino. Skill levels in specific seasons and regions could benefit users who understand the aspects of the seasonal forecasts sufficiently for prudent decision making for their application. Therefore, assessments of the seasonal forecasts for more specific regions and/or seasons are also necessary for further study.


• Some important references:

Min YM, Kryjov VN, Park CK (2009) A probabilistic multimodel ensemble approach to seasonal prediction. Wea Forecasting 24: 812-828. doi:10.1175/2008WAF2222140.1

Min YM, Kryjov VN, Oh SM (2014) Assessment of APCC multimodel ensemble prediction in seasonal climate forecasting: Retrospective (1983–2003) and real-time forecasts (2008–2013). J Geophys Res 199:12132–12150